Journal of **N**onlinear **A**nalysis and **O**ptimization
Vol. 16, Issue. 1: 2025
ISSN : **1906-9685**

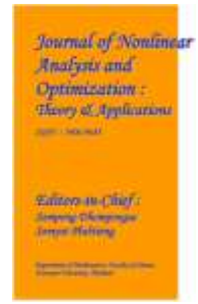

Active Converter Injection-based Protection for a Photovoltaic DC Distribution System

[1]Dr.S.Selvakumar Raja, [2]Mr.B.Mahendar

[1]Principal & Professor Department of ECE, Kakatiya Institute of technology and science for women, Manikbhandar, Nizamabad-503003, Telangana State, India

[2]HOD, EEE Department of EEE, Kakatiya Institute of technology and science for women, Manikbhandar, Nizamabad-503003, Telangana State, India

Abstract: **Because of the intricate construction of flexible DC conveyance frameworks with dispersed photovoltaic control, single-ended estimation Based security is ineffective. Additionally, the short time range with blaming features makes it difficult to identify the DC line-to-line faults. That's influenced by different converter structures and control calculations. To resolve these issues, an unused blame discovery and area strategy based on dynamic converter infusion is displayed. The proposed strategy adjusts the converter to end up a frequency-controllable infusion source by effectively utilizing the facilitated control between nearby assurance and the converters, which can construct a clear security boundary. In addition, this strategy can find the blamed zone precisely by selecting the fitting infused consonant recurrence; The DC/DC converter's outlet capacitance and the cable-distributed capacitance have an impact on this. Comparatively with current DC security methods, this strategy does not require extra infusion hardware and tall information inspecting recurrence. Equipment tests and reenactment comes about are carried out, outlining that the proposed component is successful to attain both control and security through the controllability of control gadgets.**

Keywords—Flexible DC distribution system, Distributed photovoltaic, Frequency characteristics, Harmonic impedance, Active protection.

I. INTRODUCTION

The design and analysis of distributed and multi-terminal DC power systems has been extensively researched. In contrast with the current AC grid, they provide several benefits, such as increased power quality, dependability, and energy efficiency [1–3]. Additionally, by facilitating a high penetration of distributed renewable energy and DC demands, DC distribution systems might help future smart grids [4–7]. However, the inability to accurately identify faults, locate fault areas, isolate fault areas quickly, and establish clear rules and guidelines compromises the defense of DC distribution systems with many terminals. Versatile DC systems for distribution have both converters between DC and DC and voltage source converters (VSCs). Different converter structures place different demands on the system protection performance: two-level VSCs, modular multilevel converters (MMCs), and direct current transformers (DCTs) are examples of converters that are vulnerable to DC faults in the absence of additional fault current limiters or DC circuit breakers [8]. Because of its powerful fault current blocking capabilities, the CDSM-MMC (Clamp Doubles Sub-Module Modular Multilevel Converter) architecture is used in

several contemporary projects in conjunction with DAB (Dual Active Bridge Unit Transformer) [9][10]. The primary protection issue in this situation is that the system is unable to produce useful fault information for protection when a DC fault happens between the lines (pole-to-pole) because the high fault current stops the converter in 1-2 mille seconds. There are two types of algorithms designed to safeguard DC systems: passive and active. The passive techniques can be further divided into single-sided protection and double-sided protection based on whether a communication channel and distant end information are needed. In the former scenario, local measurements are the only way to identify the problematic line. Rapidly fluctuating DC residual currents have been satisfactorily detected using voltage leakage-based protection techniques, leakage current (di/dt and d2i/dt2), and under voltage [11][12]. These techniques, however, compromise the selectivity of relay functioning and do not offer a clearly defined limit. In order to satisfy the selectivity criteria, [13] uses The rate of voltage change at the containment reactor as the protection criterion. However, the DC side reactor may have an effect on the VSC-DC distribution's dynamic performance. In conclusion, it is challenging to detect every flaw on the line of protection in 1-2 ms due to the absence of a specified limit in single-ended measurement-based protection. To provide a clear protected area, a number of double-sided protection algorithms have been put forth. Differential protection [14][15] is the most straightforward of these, however reliability may be impacted by transient currents in the line distribution capacitance. Low-pass filters have an impact on the protection speed but can remove transient currents from line-dispersed capacitors. In [16], a third study suggests pilot protection using transient voltages. In DC-limiting reactors, and another event-based prevention technique in [17] uses communication to discover errors in the current rate of change. Although both forms of protection operate satisfactorily, they are only applicable in systems with a restricted reactor.

Furthermore, the majority of active techniques have been suggested for DC networks with low and medium voltages. Installing extra devices and recording certain signal inputs are active ways [18–21] for locating and detecting faults. The primary disadvantage is that, for reliability concerns, the power provider might not permit extra equipment. Furthermore, there is a chance that the localization findings will give false fault spots because of the intricate branch structure of DC distribution networks. As a result, creating new protection principles with high dependability and selectivity is crucial. This study suggests a novel fault localization and detection technique to offer active protection for multi-pole photovoltaic (PV) flexible DC distribution systems in light of these problems. This paper's primary contributions are:

The suggested approach turns converters into injection sources with known characteristic signals for protection by utilizing local protection and coordinated control among converters in the system.

The majority of current DC protection systems concentrate on identifying problematic line segments, but pinpointing the precise fault site for fault correction still takes a very long time. The recommended protection method may identify the fault and isolate the fault line while eliminating the DC fault by figuring out the harmonic impedance of these distinctive signals. This significantly reduces the system recovery time. By contrasting the suggested protection's performance with that of current approaches, we demonstrate that the suggested method outperforms them and doesn't call for additional injection tools or changes to the setup across the system.

II. EXAMINATION FROM THE PROCESS OF A CONVERTER FAULTS

A multi-connected DC distribution system [22] was the basis for the application project that was selected as the study topic (Figure 1). A DAB raises six solar plants' on-site voltage to ±10 kV. A ring system is created by connecting the plants using DC wires. A high-frequency transformer and an H-bridge on each side make up the DAB. By altering the pulse width of the H-bridge, the voltage level on either side of the DAB can be changed, and the high-frequency transformer serves as an electrical isolation device. Bidirectional power transfer between the AC and DC systems is thus made possible by the CDSM-MMC, which links the ring system to the AC system. In typical operation, the DAB works similarly to a power supply, and the AC/DC converter uses continuous DC voltage regulation on the DC side. To balance the energy produced by solar cells. Two additional energy storage devices are part of the system. At the output of each PV terminal, a current-limiting reactor is installed concurrently to safeguard the converter equipment in the event that the DC switch cuts the fault current. Converter communication allows for the protection and control of the multi-pole DC distribution system. It is possible to modify the local converter's modulation frequency through device-level control (DC/DC converter control).

A communication network (Generic Object-Oriented Substation Events or GOOSE technology that facilitates information exchange between transducers and local protection makes it possible for several transducers to coordinate and function together. Thus, following a defect, the local transducer may be transformed into an injection source with a distinct frequency signal by altering its modulation frequency. In practice, the neutral point on the DC side is usually connected to ground via high impedance [23]. If there is a connection-to-ground failure, clamping the fault line to zero voltage. The power transformer sub module's capacitors help raise the healthy pole's voltage to double its pre-fault level while maintaining a steady voltage between the poles [24]. Therefore, line-to-earth faults are protected from DC voltage imbalance and over current damage is not caused by DC line-to-earth faults. Therefore, our work is mostly focused on line-to-line DC faults.

A Features of the CDSM-MMC Fault

The "detection phase" and "isolation phase" of a DC line fault are the two stages into which the CDSM Figure 2 shows how the fault progression time can be used to differentiate MMC's fault transition.

Stage 1:

As seen in Figure 2(a), the analogous circuit during the "detection phase" is a quadratic function of the solid-state defect. Under the circumstances, the circuit's normal reaction oscillates$R < 2\sqrt{L/C}$, where L stands for the bridge branch reactor's equivalent inductance, C for the converter's equivalent capacitance, and R for the capacitor's series resistance and the converter's contact resistance.

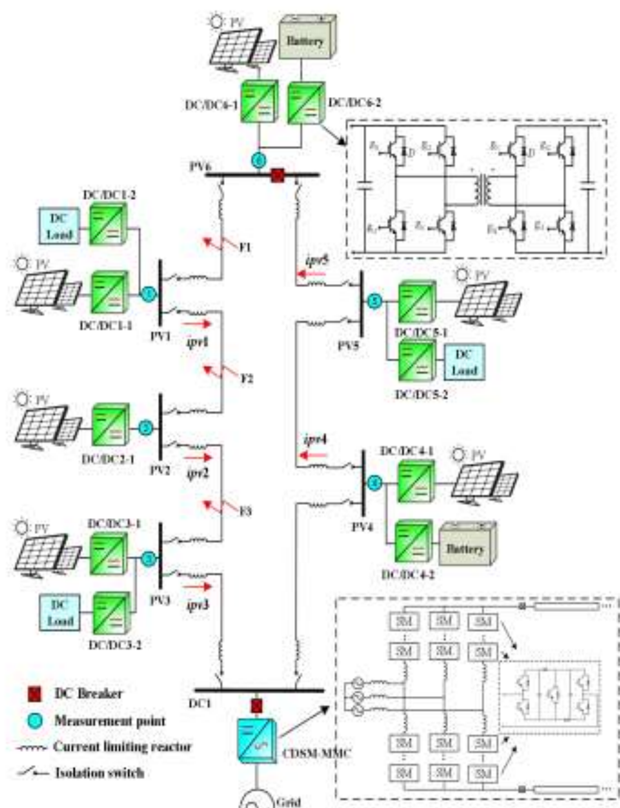

Fig. 1: Architecture of a flexible multi-terminal DC distribution system

Discharge circuit.

Equivalent sub module

The following is the expression for the natural response when the load current is set to I0 and the capacitor voltage is set to Udc.

$$
\begin{cases}
i_{dc}(t) = (U_{dc}/\omega L)e^{-\delta t}\sin(\omega t) - (I_0\omega_0/\omega)e^{-\delta t}\sin(\omega t - \beta) \\
u_C(t) = (U_{dc}\omega_0/\omega)e^{-\delta t}\sin(\omega t + \beta) - (I_0/C\omega)e^{-\delta t}\sin(\omega t) \\
\beta = \arctan(\omega/\delta)
\end{cases} \quad (1)
$$

Stage 2:

Following the converter's blocking, the "isolation stage" involves the directing potential to the fault circuit provided by the series/parallel capacitance voltage. As seen in Figure 2(b), the fault current at the bridge branch travels in two distinct directions. The lower bridge branches' phases A and C make up fault route 2, whereas the higher bridge branches' phases A and B make up fault path 1. In order to bring the fault current down to zero during the fault isolation stage, the sub module capacitors must receive all of the current. The voltage of the capacitor increases at the same time.

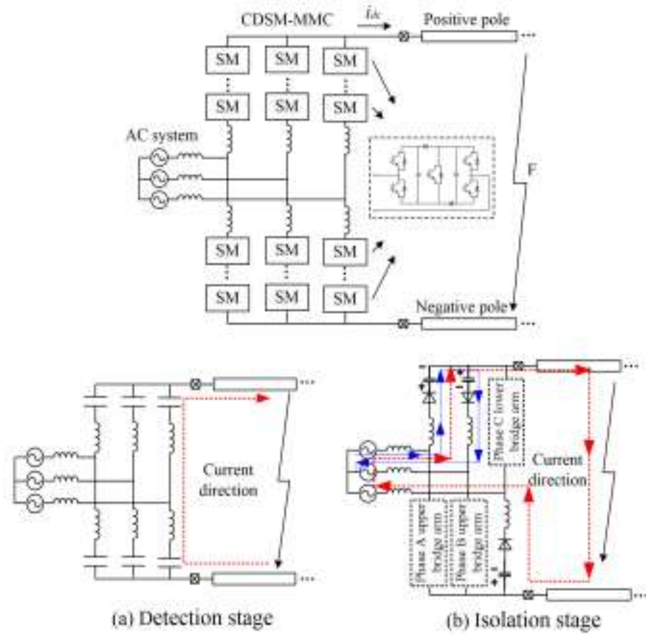

Fig. 2 CDSM-MMC equivalent circuits at various phases of the failure

B. Fault Characteristics of DAB

A DC fault's "detection phase" and "isolation phase" are the two distinct stages that make up the fault transient. in spite of the DAB converter's performance, depending on how long a pole-top defect takes to propagate. The on-site PV voltage step-up transformer's DC/DC module is thought to have a single DAB sub module. Figure 3 depicts the analogous circuit with a pole-to-pole failure on the DC line.

Stage 1:

Because of the significant voltage differential between the output capacitor and the fault site, energy stored in the output When there is pole-to-pole DC malfunction, the capacitor is rapidly released to the fault location. It takes very little time for the current to reach its maximum. This process is hence also known as the capacitor discharge operation. The circuit is comparable to an RLC tank circuit, and the route is depicted in Figure 3's first row [25]. To put it another way, the circuit is responding under damped.

Stage 2:

The current rapidly rises to the DAB's IGBTs' (Insulated Gate Bipolar Transistors) self-protection value. The DC/DC transformer is then blocked. By cutting off the fault current, a continuous flow channel is formed through the reactor and the anti-parallel diodes of the H-bridge. The path is shown in the second row in Figure 3. The DC fault current progressively decreases to zero once the DAB is turned off because the high-frequency transformer in the DAB module is electrically disconnected.

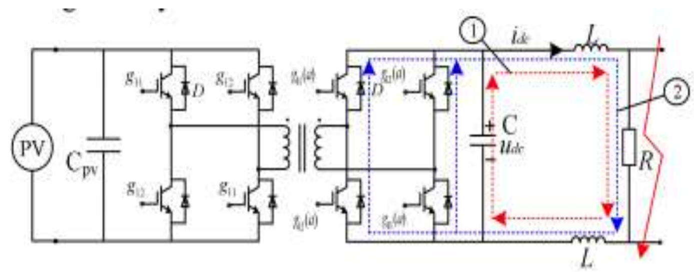

Fig. 3. DAB comparable circuits in case of a failure from pole to pole

According to the fault process analysis, since the DC cable fault current is zero, the isolation step—which is a part of both CDSM-MMC and DAB—cannot supply fault transient information for protection. After the issue arises, The frequency at which the converter modulates is changed to modify the converter control and inject a characteristic signal. To find and identify the problem, these distinct signals are computed and picked up.

III. A PROTECTION METHOD ACTIVE CONVERTERINJECTION BASED ON

A. Where the Single-end Fault Distance Is

At a predetermined frequency, the DAB uses a square wave pulse-width modulation (PWM) signal to turn on and off the In the H-bridge are IGBTs. The output frequency and the DAB's switching frequency fluctuate in unison when using the conventional PWM control approach is dictated by the PWM signal's frequency. The PWM trigger pulse's frequency is altered in this work to alter the DAB's switching frequency, enabling the DAB to produce a predetermined amount of intrinsic harmonic content. One way to think of the DAB's output frequency is as a self-defined harmonic source. H-bridge IGBTs. The output frequency and the switching frequency of the DAB change in unison when using the conventional PWM control approach the capacitor in the DAB gradually reaches a new stable condition. Its equivalent circuit is depicted in Figure 4, where udc is the output's capacitor voltage, Co is the output's equivalent capacitance, and CPV is the equivalent capacitance of the DAB's low-voltage side. The DC line's equivalent the symbols Ll and Rl stand for inductance and resistance, respectively, and Rf for fault resistance. The capacitor CPV (route ①) is charged by the PV power source (constant current source), as shown in Figure 4 in the process of energy flow. In addition to charging the output capacitor Co, the capacitor CPV then uses the DAB to power the issue site. Figure 4 shows the blue arrow for the current route, which comprises the connections of CPV, g11, g11', and Co. Connecting CPV, g12, g12', and Co, the alternate route is indicated by the red arrow. A fault loop circuit (route ②) is produced by the DAB's output capacitor in conjunction both the fault resistor and the DC fault line are involved.

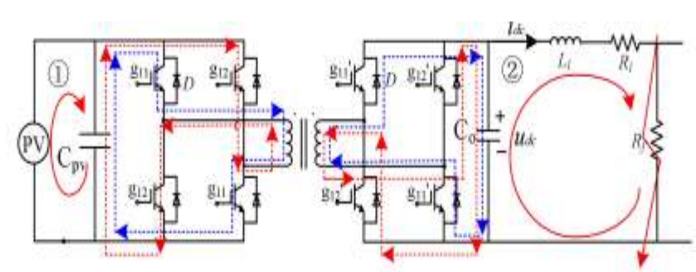

Fig. 4. Equivalent steady-state circuits following a failure

Furthermore, it may be claimed that the external environment remains stable throughout the harmonic current injection of DAB because both the output capacitor's voltage differential and the energy it stores are now quite modest. There is no change in the PV output's characteristics. Because the PV side use the MPPT control mechanism, the output current of the PV is fixed. During DAB unlocking, the fault circuit will swiftly move to a new stable condition because to the low fault current. Consequently, the PV as well as DAB sources can be considered sources of harmonic injection. Once the fault F2 example (Figure 1) has been used to examine the fault circuit's impedance, Figure 5 shows the added harmonic current loop.R1 and The inductance of the current-limiting reactor is L0, and the resistance and inductance of the DC are L1. At measurement point 6, the line voltage and current are upv6 and ipv6, respectively, along with the cable per kilometer (Figure 1). The length of the DC connection between PV1 and PV6 is denoted by x in Figure 1, whereas y1 represents the distance between measurement point 1 as well as fault site F2. DC/DC1-2 and DC/DC1-1 output capacitors are denoted by the symbols C1-1 and C1-2, respectively.

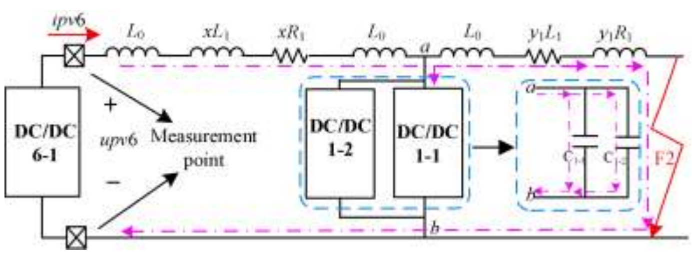

Fig. 5 DC fault including a loop of injected harmonic current

Once a harmonious current is switched via the DC wire between the fault points F2, DC/DC1-1, and DC/DC1-2 and the measuring point, the current flows via DC/DC6-1 in Figure 5. The output capacitor is the only component that permits the harmonic current to flow because DC/DC1-1 and DC/DC1-2 are blocked. A display of the recorded DC side voltage upv6 in the frequency range is shown in Figure 5:

$$U_{pv6}^{f} = xR_1 I_{pv6}^{f} + j2\pi f(xL_1 + 2L_0)I_{pv6}^{f} + \{[1/(j2\pi f C_{1-1})] \\ //[1/(j2\pi f C_{1-2})]//[y_1R_1 + j2\pi f(y_1L_1 + L_0)]\}I_{pv6}^{f} \qquad (2)$$

Upv6f and Ipv6f are the harmonic vectors of the observed voltage and current, respectively, while f is the frequency (DAB switching frequency). By employing a parallel input-output series structure (IPOS), as illustrated in Figure A1 of the Appendix, the DAB raises the solar power plant's capacity and voltage. As a result, the output's equivalent capacitance of the DAB is reduced. The DC/DC converter output's harmonic impedance is therefore significantly higher than the DC line's impedance. Thus, it is possible to ignore the DAB's impedance and have very minimal harmonic current flow in DC/DC1-1 and DC/DC1-2. Consequently, (2) can be lowered to

$$U_{pv6}^{f} = xR_1 I_{pv6}^{f} + j2\pi f(xL_1 + 2L_0)I_{pv6}^{f} + \\ [y_1R_1 + j2\pi f(y_1L_1 + L_0)]I_{pv6}^{f} \qquad (3)$$

The measured impedance Z_pvδ f and fault distance can be found in three (3) states by

$$Z_{pv6}^{f} = U_{pv6}^{f} / I_{pv6}^{f} = j2\pi f 3L_0 + (R_1 + j2\pi f L_1)(x + y_1) \quad (4)$$

$$x + y_1 = (Z_{pv6}^{f} - j2\pi f 3L_0)/(R_1 + j2\pi f L_1) \quad (5)$$

It should be noted that the DAB's impedance cannot be disregarded whether there is an unusually high switching harmonic frequency or if the system's properties deviate from those outlined in this study. Nevertheless, (2) may be used to compute the error distance. A key component of the suggested fault finding technique is the precise extraction of the harmonic content from the readings. As a result, the defect is promptly located using a windowed Fourier technique (about one cycle of the user-defined frequency).

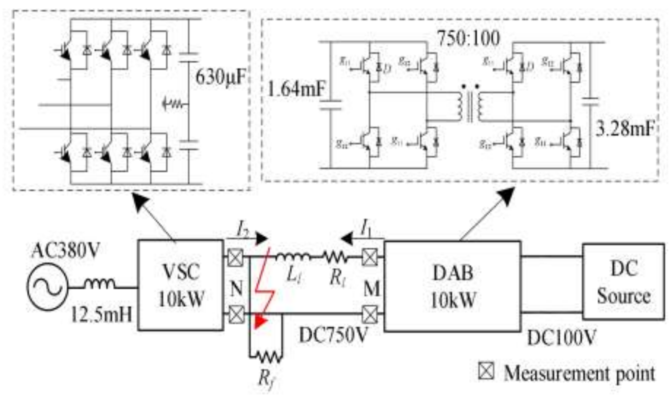

Fig. 6 Topology of VSC-DC system with DAB

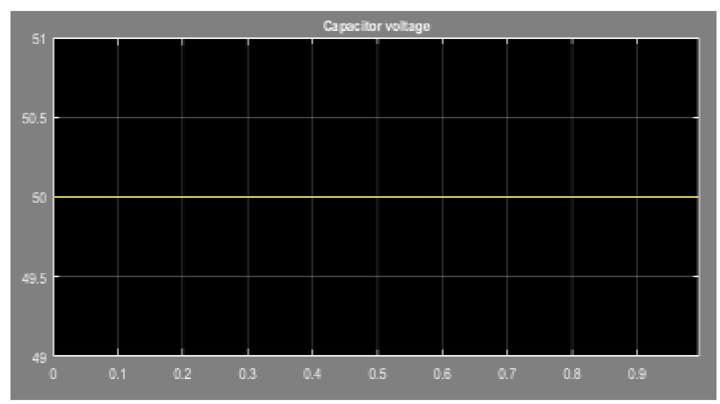

(a)

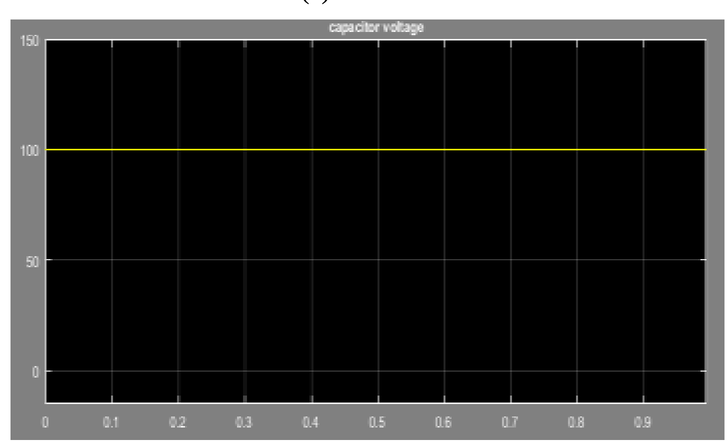

(b)

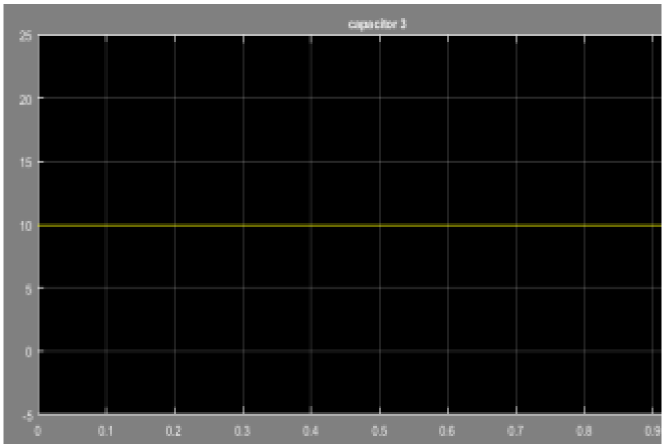

(c)

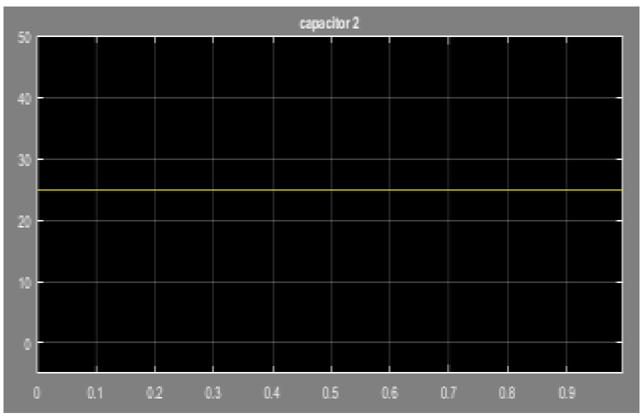

(d)

Fig. 7 Waveform of DC current in steady condition with varying DAB switching frequencies

In Figure 6, Point M is where the voltage waveform is monitored. The steps involved in altering the DAB switching frequency are shown in Fig. 7. so that the output voltage frequency and current may be verified in respect to the switching frequency.

IV.CONCLUSIONS

An active protection approach for adaptable DC distribution networks is presented in this paper using multi-terminal distributed PV Results from hardware testing and simulations show that the technique can successfully combine protection and control through power electronics controllability and precisely pinpoint the issue location with the appropriate injected harmonic frequency selection. This solution does not require a high frequency of data collection or extra injection equipment, in contrast to the DC protection strategy that was previously explained. Furthermore, neither measurement noise nor cable distribution capacitance affect the proposed technique. As a result, a vast and intricate industrial DC network may benefit from the increased security.

REFERENCES

[1] Q. Song, B. Zhao, J. Li and W. Liu, "An Improved DC Solid State Transformer Based on Switched Capacitor and Multiple-Phase-Shift Shoot-Through Modulation for Integration of LVDC Energy Storage System and MVDC Distribution Grid," IEEE Transactions on Industrial Electronics, vol. 65, DOI 10.1109/TIE.2017.2786198, no. 8, pp. 6719-6729, Aug. 2018.

[2] A. Egea-Alvarez, F. Bianchi, A. Junyent-Ferre, G. Gross and O. Gomis-Bellmunt, "Voltage control of multi terminal VSC-HVDC transmission systems for offshore wind power plants: Design and implementation in a scaled platform", IEEE Transactions on Industrial Electronics, vol. 60, DOI 10.1109/TIE.2012.2230597, no. 6, pp. 2381-2391, Jun. 2013.

[3] Y. Wang, Q. Song, Q. Sun, B. Zhao, J. Li and W. Liu, "Multilevel MVDC Link Strategy of High-Frequency-Link DC Transformer Based on Switched Capacitor for MVDC Power Distribution," IEEE Transactions on Industrial Electronics, vol. 64, DOI 10.1109/TIE.2016.2643622, no. 4, pp. 2829-2835, April 2017.

[4] K. Jia, R. Zhu, T. Bi, Q. Zhao, C. Wang and Z. Xuan, "Fuzzy-Logic-Based Active Protection for Photovoltaic DC Power Plant," IEEE Transactions on Power Delivery, vol. 35, DOI10.1109/TPWRD.2019.2907115, no. 2, pp. 497-507, April 2020.

[5] Yuanpeng Guan, Yunxiang Xie, Yu Wang, Yi Liang, Xuemei Wang, "An Active Damping Strategy for Input Impedance of Bidirectional Dual Active Bridge DC–DC Converter: Modeling Shaping Design and Experiment", IEEE Transactions on Industrial Electronics, vol. 68, DOI10.1109/TIE.2020.2969126, no. 2, pp. 1263-1274, 2021.

[6] Lu, K. Sun, J. M. Guerrero, J. C. Vasquez and L. Huang, "State-of-charge balance using adaptive droop control for distributed energy storage systems in DC micro grid applications", IEEE Transactions on Industrial Electronics, vol. 61, no. 6, pp. 2804-2815, Jun. 2014.

[7] K. Park and Z. Chen, "A double uneven power converter-based dc-dc converter for high-power dc grid systems", IEEE Transactions on Industrial Electronics, vol. 62, DOI 10.1109/TIE.2015.2458301, no. 12, pp. 7599-7608, Dec. 2015.

[8] Yang, J. Fletcher and J. O'Reilly, "Short-circuit and ground fault analyses and location in VSC-based DC network cables", IEEE Transactions on Industrial Electronics, vol. 59, DOI 10.1109/TIE.2011.2162712, no. 10, pp. 3827-3837, Oct. 2012.

[9] J. -Y. Lee, H. -S. Kim and J. -H. Jung, "Enhanced Dual-Active-Bridge DC – DC Converter for Balancing Bipolar Voltage Level of DC Distribution System," IEEE Transactions on Industrial Electronics, vol. 67, DOI 10.1109/TIE.2019.2959503, no. 12, pp. 10399-10409, Dec. 2020.

[10] J. Yang, J. Liu, J. Zhang, N. Zhao, Y. Wang and T. Q. Zheng, "Multi rate Digital Signal Processing and Noise Suppression for Dual Active Bridge DC–DC Converters in a Power Electronic Traction Transformer," IEEE Transactions on Power Electronics, vol. 33, DOI 10.1109/TPEL.2018.2803744, no. 12, pp. 10885-10902, Dec. 2018.

[11] X. Feng, L. Qi and J. Pan, "A Novel Fault Location Method and Algorithm for DC Distribution Protection," IEEE Transactions on Industry Applications, vol. 53, DOI 10.1109/TIA.2017.2666083, no. 3, pp. 1834-1840, May-June 2017.

[12] A. Meghwani, S. C. Srivastava and S. Chakrabarti, "A Non-unit Protection Scheme for DC Micro grid Based on Local Measurements," IEEE Transactions on Power

Delivery, vol. 32, DOI 10.1109/TPWRD.2016.2555844, no. 1, pp. 172-181, Feb. 2017.

[13] R. Li, L. Xu and L. Yao, "DC Fault Detection and Location in Meshed Multi terminal HVDC Systems Based on DC Reactor Voltage Change Rate," IEEE Transactions on Power Delivery, vol. 32, DOI 10.1109/TPWRD.2016.2590501, no. 3, pp. 1516-1526, June 2017.

[14] S. Dhar, R. K. Patnaik and P. K. Dash, "Fault Detection and Location of Photovoltaic Based DC Micro grid Using Differential Protection Strategy," in IEEE Transactions on Smart Grid, vol. 9, DOI 10.1109/TSG.2017.2654267, no. 5, pp. 4303-4312, Sept. 2018.

[15] S. D. A. Fletcher, P. J. Norman, K. Fong, S. J. Galloway and G. M. Burt, "High-Speed Differential Protection for Smart DC Distribution Systems," IEEE Transactions on Smart Grid, vol. 5, DOI 10.1109/TSG.2014.2306064, no. 5, pp. 2610-2617, Sept. 2014.

[16] J. Liu, N. Tai and C. Fan, "Transient-Voltage-Based Protection Scheme for DC Line Faults in the Multi terminal VSC-HVDC System," IEEE Transactions on Power Delivery, vol. 32, DOI 10.1109/TPWRD.2016.2608986, no. 3, pp. 1483-1494, June 2017.

[17] M. Farhadi and O. A. Mohammed, "Event-Based Protection Scheme for a Multi terminal Hybrid DC Power System," IEEE Transactions on Smart Grid, vol. 6, DOI 10.1109/TSG.2015.2396995, no. 4, pp. 1658-1669, July 2015.

[18] S. Kim, S. Kim and D. Dujic, "Extending Protection Selectivity in DC Shipboard Power Systems by Means of Additional Bus Capacitance," IEEE Transactions on Industrial Electronics, vol. 67, no. 5, pp. 3673-3683, May 2020.

[19] K. Jia, E. Christopher, D. Thomas, M. Sumner and T. Bi, "Advanced DC zonal marine power system protection," IET Generation, Transmission & Distribution, vol. 8, DOI 10.1049/iet-gtd.2013.0139, no. 2, pp. 301-309, February 2014.

[20] E. Christopher, M. Sumner, D. Thomas and F. de Wildt, "Fault location for a DC zonal electrical distribution system using active impedance estimation," 2011 IEEE Electric Ship Technologies Symposium, Alexandria, VA, 2011, pp. 310-314.

[21] J. Chen et al., "DC-side fault detection for photovoltaic energy conversion system using fractional-order dynamic-error-based fuzzy Petri net integrated with intelligent meters," IET Renewable Power Generation, vol. 10, DOI 10.1049/iet-rpg.2015.0517, no. 9, pp. 1318-1327, Oct. 2016.

[22] K. Jia, Q. Zhao, T. Feng and T. Bi, "Distance Protection Scheme for DC Distribution Systems Based on the High-Frequency Characteristics of Faults," IEEE Transactions on Power Delivery, vol. 35, DOI 10.1109/TPWRD.2019.2909130, no. 1, pp. 234-243, Feb. 2020.

[23] M. Li, K. Jia, T. Bi and Q. Yang, "Sixth harmonic-based fault location for VSC-DC distribution systems," IET Generation, Transmission & Distribution, vol. 11, DOI 10.1049/iet-gtd.2016.1865, no. 14, pp. 3485-3490, 9 28 2017.

[24] M. Wang, W. Leterme, G. Chaffey, J. Beerten and D. Van Hertem, "Pole Rebalancing Methods for Pole-to-Ground Faults in Symmetrical Monopolar HVDC Grids," IEEE Transactions on Power Delivery, vol. 34, DOI 10.1109/TPWRD.2018.2853704, no. 1, pp. 188-197, Feb. 2019.

[25] K. Jia, C. Wang, T. Bi, T. Feng and R. Zhu, "Transient Current Correlation Based Protection for DC Distribution System," IEEE Transactions on Industrial Electronics, vol. 67, DOI 10.1109/TIE.2019.2952805, no. 11, pp. 9927-9936, Nov. 2020.